

Janus Particles at Liquid–Liquid Interfaces

Nicole Glaser,[†] Dave J. Adams,[‡] Alexander Böker,^{*,†} and Georg Krausch^{*,†}

Lehrstuhl für Physikalische Chemie II and Bayreuther Zentrum für Kolloide und Grenzflächen (BZKG), Universität Bayreuth, 95440 Bayreuth, Germany, and Unilever Corporate Research, Colworth, U.K.

Received March 14, 2006

Following recent theoretical predictions, we report on the first experiments on the interfacial activity of so-called Janus nanoparticles (i.e., bifacial particles consisting of a gold and an iron oxide moiety). Using pendant drop tensiometry, we show that the amphiphilicity derived from the Janus character of the particles leads to a significantly higher interfacial activity compared to that of the respective homogeneous particles of the same size. The self-assembly of Janus particles at the hexane–water interface results in a significant decrease in the interfacial tension. Furthermore, we demonstrate control over the interfacial activity by tuning the particles' amphiphilicity via ligand-exchange reactions.

Introduction

In recent years, the controlled synthesis of nanoparticles has become an area of increasing interest because of their outstanding optical, electronic, and magnetic properties. At the beginning of the last century, Pickering discovered the stabilizing effect of such particles in emulsions.¹ The first theoretical description of this effect was presented by Pieranski.² Recently, Lin et al. have shown that organic and inorganic nanoparticles assemble at liquid interfaces forming well-defined monolayers that can serve as building blocks for nanoporous capsules and membranes.^{3–6} Recent theoretical considerations by Binks predict that the stabilization of Pickering emulsions should be considerably improved when so-called Janus particles instead of homogeneous particles are used.⁷ In contrast to a particle exhibiting uniform wettability, the surface of a Janus particle is compartmentalized and has two parts exhibiting different wettability. Therefore, a truly amphiphilic particle that combines the typical Pickering effect and the amphiphilicity of a classical surfactant can result. In consequence, a considerable increase in surface activity is expected. Different routes to obtain Janus particles have been explored in the recent past.^{8–17} Some of the approaches^{8–13} are based on amphiphilic block copolymers. They suffer from a

rather complicated preparation process and the difficulty of clearly establishing the Janus character of the resulting objects. Janus particles have also been obtained via inorganic synthesis, including acorn-like particles made of PdS_x/Co₉S₈¹⁴ or dumbbell-like particles made of CdS/FePt¹⁵ and Ag/CoFe₂O₃.¹⁶ Lately, Duguët et al. have reported the synthesis of silica particles with two hemispheres covered by different ligands via protection and deprotection of a fraction of the particle via PS beads.¹⁷ These approaches seem more appealing because the synthesis is rather straightforward and the Janus character of the particles can often be directly visualized by electron microscopy. However, to best of our knowledge, the interfacial activity of such Janus particles has not yet been investigated, and the predicted advantage of Janus particles versus homogeneous particles for the stabilization of a Pickering emulsion remains to be demonstrated.

Results and Discussion

In the present work, we aim to provide an experimental confirmation of Binks' theoretical prediction.⁷ We synthesized Janus particles made of an Au and an Fe₃O₄ part following a route first described by Yu et al.¹⁸ The synthesis is based on the controlled nucleation and epitaxial growth of a single iron oxide particle onto the surface of a single-crystalline gold seed acting as a precursor. The results of the synthesis were followed by transmission electron microscopy (TEM). The specimens for TEM analysis were prepared by room-temperature deposition of a hexane dispersion containing the nanoparticles onto carbon-coated copper grids. TEM images were acquired using a Zeiss 902 electron microscope operated at 80 kV. In Figure 1a, such Janus particles are shown. The mean diameter of the gold particle is around 4 nm, and the diameter of iron oxide is about 10 nm, resulting in an overall diameter of about 14 nm. (The diameters were determined by the image analysis program package Image J.¹⁹) In addition, the size of the particles was measured by dynamic light scattering, revealing similar results (not shown here).

To establish the effect of the Janus character of the particles on their interfacial activity, homogeneous nanoparticles of both

* Corresponding authors. E-mail: alexander.boeker@uni-bayreuth.de, georg.krausch@uni-bayreuth.de.

[†] Universität Bayreuth.

[‡] Unilever Corporate Research.

(1) Pickering, S. J. *Chem. Soc.* **1907**, 91, 307.

(2) Pieranski, P. *Phys. Rev. Lett.* **1980**, 45, 569–572.

(3) Lin, Y.; Skaff, H.; Böker, A.; Dinsmore, A. D.; Emrick, T.; Russell, T. P. *J. Am. Chem. Soc.* **2003**, 125, 12690–12691.

(4) Lin, Y.; Böker, A.; Skaff, H.; Cookson, D.; Dinsmore, A. D.; Emrick, T.; Russell, T. P. *Langmuir* **2005**, 21, 191–194.

(5) Böker, A.; Lin, Y.; Chiapperini, K.; Horowitz, R.; Thompson, M.; Carreon, V.; Xu, T.; Abetz, C.; Skaff, H.; Dinsmore, A. D.; Emrick, T.; Russell, T. P. *Nat. Mater.* **2004**, 3, 302–306.

(6) Russell, J. T.; Lin, Y.; Böker, A.; Su, L.; Carl, P.; Zettl, H.; He, J. B.; Sill, K.; Tangirala, R.; Emrick, T.; Littrell, K.; Thiagarajan, P.; Cookson, D.; Fery, A.; Wang, Q.; Russell, T. P. *Angew. Chem., Int. Ed.* **2005**, 44, 2420–2426.

(7) Binks, B. P.; Fletcher, P. D. I. *Langmuir* **2001**, 17, 4708–4710.

(8) Perro, A.; Reculosa, S.; Ravaine, S.; Bourgeat-Lami, E. B.; Duguët, E. *J. Mater. Chem.* **2005**, 15, 3745–3760.

(9) Erhardt, R.; Böker, A.; Zettl, H.; Kaya, H.; Pyckhout-Hintzen, W.; Krausch, G.; Abetz, V.; Müller, A. H. E. *Macromolecules* **2001**, 34, 1069–1075.

(10) Erhardt, R.; Zhang, M. F.; Böker, A.; Zettl, H.; Abetz, C.; Frederik, P.; Krausch, G.; Abetz, V.; Müller, A. H. E. *J. Am. Chem. Soc.* **2003**, 125, 3260–3267.

(11) Liu, Y.; Abetz, V.; Müller, A. H. E. *Macromolecules* **2003**, 36, 7894–7898.

(12) Förster, S.; Antonietti, M. *Adv. Mater.* **1998**, 10, 195–217.

(13) Schrage, S.; Sigel, R.; Schlaad, H. *Macromolecules* **2003**, 36, 1417–1420.

(14) Teranishi, T.; Inoue, Y.; Nakaya, M.; Oumi, Y.; Sano, T. *J. Am. Chem. Soc.* **2004**, 126, 9914–9915.

(15) Gu, H. W.; Zheng, R. K.; Zhang, X. X.; Xu, B. *J. Am. Chem. Soc.* **2004**, 126, 5664–5665.

(16) Li, Y.; Zhang, Q.; Nurmikko, A. V.; Sun, S. H. *Nano Lett.* **2005**, 5, 1689–1692.

(17) (a) Duguët, E.; Poncet-Legrand, C.; Ravaine, S.; Bourgeat-Lami, E.; Reculosa, S.; Mingotaud, C.; Delville, M. H.; Pereira, F. WO 2005/049195, France, 2005. (b) Perro, A.; Reculosa, S.; Pereira, F.; Delville, M. H.; Mingotaud, C.; Duguët, E.; Bourgeat-Lami, E.; Ravaine, S. *Chem. Commun.* **2005**, 5542–5543.

(18) Yu, H.; Chen, M.; Rice, P. M.; Wang, S. X.; White, R. L.; Sun, S. H. *Nano Lett.* **2005**, 5, 379–382.

(19) For more information, see <http://rsb.info.nih.gov/ij/>.

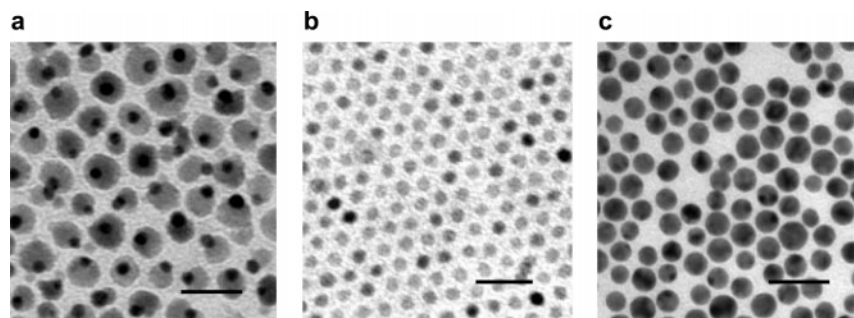


Figure 1. TEM images of the nanoparticles: (a) Janus particles (consisting of gold (darker spheres) and iron oxide (brighter spheres)); (b) homogeneous iron oxide particles; and (c) gold particles. The scale bars represent 25 nm.

gold and iron oxide of comparable sizes were synthesized as well. The synthesis of iron oxide nanoparticles followed the same route as for the Janus particles excluding the addition of the gold precursor. Oleic acid and oleylamine were used as ligands for the homogeneous iron oxide nanoparticles as well as the iron oxide part of the Janus particles. The preparation of the gold nanoparticles was similar to the synthesis described by Yu et al.;¹⁸ however, the solution was heated to 120 °C instead of 65 °C. At 120 °C, the solution turned dark red. After that, the reaction mixture was stirred for an additional 4 h at 65 °C to ensure complete reaction. Parts b and c of Figure 1 show TEM micrographs of the resulting iron oxide and gold nanoparticles, respectively. Homogeneous nanoparticles have a slightly smaller diameter than the Janus-type particles synthesized for this study. The gold nanoparticle diameter is about 10 nm, and the iron oxide nanoparticle diameter is about 7 nm. To increase the amphiphilic character of the Janus particles further, dodecanethiol (DDT) and octadecanethiol (ODT) molecules were attached to the gold part via ligand exchange. The resulting solution mixture was centrifuged with ethanol to remove excess thiol. During this process, the ligands at the iron oxide part were removed as well. The successful exchange reaction and the removal of oleic acid were monitored by IR spectroscopy and thermogravimetric analysis (Supporting Information). Both ligands are expected to increase the hydrophobic character of the gold part within the Janus particle, thereby leading to an overall increase in the amphiphilic character of the particles. For quantitative comparison, the homogeneous gold nanoparticles were also capped with DDT following the same procedure as for the Janus particles.

The surface activity of the nanoparticles was measured by the pendant drop method using a Dataphysics OCA 20 tensiometer. All measurements were performed at room temperature. Water was used as the drop phase, and *n*-hexane was used as the ambient phase in which the nanoparticles were dispersed. The concentration of nanoparticles in solution was about 1.2×10^{-4} mmol/L (i.e., 7×10^{16} nanoparticles/L). As soon as a water droplet is formed, the water/*n*-hexane interfacial tension starts to decrease as particles segregate to the interface. Eventually, the interfacial tension approaches a new equilibrium value. For the homogeneous particles, similar values of the interfacial tension are found after 1000 s (Fe₃O₄: 34.5 mN/m; Au: 33 mN/m (Figure 2)). These values are lower than for the interface between pure *n*-hexane and water, which was measured as a reference in the absence of surface-active agents.

For the Janus particles modified with DDT (JP_{DDT}), the interfacial tension drops to 22.5 mN/m. This value is significantly lower than for the homogeneous nanoparticles. As expected, the Janus particles are considerably more effective in reducing the interfacial tension. To exclude any particle shape effects on the interfacial tension, a comparison with particles of identical shape

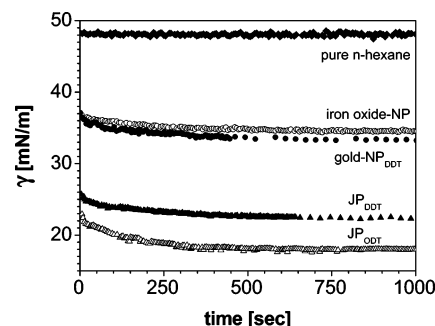


Figure 2. Interfacial tension vs time. Water was used as the drop phase, and *n*-hexane was used as the ambient phase in which the nanoparticles were diluted. (NP: homogeneous nanoparticles; JP: Janus particles. The gold moieties were modified using dodecanethiol (DDT) or octadecanethiol (ODT).)

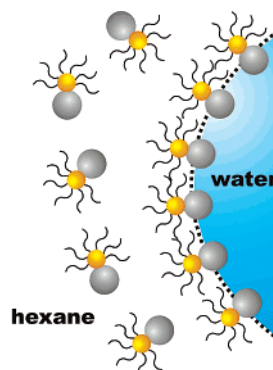


Figure 3. Schematic representation of Janus particles at the hexane–water interface (red: gold part; gray: iron oxide part).

would be desirable. Such particles consisting of SiO₂ capped with different ligands were recently synthesized by Perro et al.¹⁷ However, we do not expect a significant particle shape influence because the gold part is by far smaller than the iron oxide moiety. From the above-mentioned findings, we conclude that the Janus particles orient at the liquid/liquid interface. Because of its more nonpolar character, the hydrocarbon ligand-covered gold part should point to the hexane phase, and the more polar iron oxide should be (partially) immersed in the water phase (scheme in Figure 3). We note, however, that a direct observation of the assumed alignment of the Janus particles as well as their position with respect to the interface is still lacking.

If DDT (C₁₂H₂₅SH) is replaced by ODT (C₁₈H₃₇SH), then the hydrophobic character of the gold part of the Janus particles should be increased further, in turn leading to the yet larger amphiphilic character of the Janus particle. As can be seen in Figure 2, the longer hydrocarbon chain indeed causes a still higher surface activity of the Janus particles. The interfacial tension reaches a minimum value of as low as 18 mN/m for the

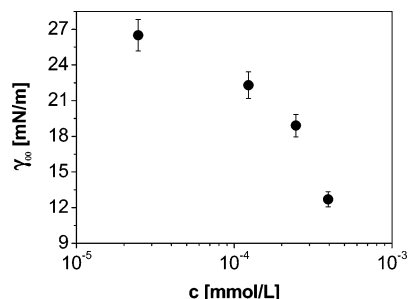


Figure 4. Equilibrium interfacial tension γ_{∞} as a function of particle concentration (DDT-capped Janus particles in *n*-hexane).

ODT-capped Janus particles as compared to the value of 22.5 mN/m reported above for the DDT-capped Janus particles.

In addition, we determined the dependence of the interfacial tension γ_{∞} (taken at $t = 1000$ s) on the concentration of the DDT-capped Janus particles. The data shown in Figure 4 reveal a distinct decrease in γ_{∞} with increasing particle concentration. The lowest value measured is around 12 mN/m at a particle concentration of 3.9×10^{-4} mmol/L (a concentration that is approximately 4 orders of magnitude lower than for typical molecular surfactants, e.g., AOT). The measurements were limited

to these rather low concentrations because more highly concentrated solutions were too absorbent for image processing.

Conclusions

In summary, we have qualitatively confirmed Bink's theoretical prediction of the effect of Janus particles at liquid–liquid interfaces. It was shown that Janus particles are considerably more active than homogeneous particles of comparable size and chemical nature. We have further shown that the interfacial activity can be increased by increasing the amphiphilic character of the particles. The results indicate the significant advantages of Janus particles in the stabilization of emulsions and foams.

Acknowledgment. We appreciate inspiring discussions with Michael Butler (Unilever Corporate Research, Colworth, U.K.). We thank Andreas Walther for the DLS measurements and Jiayin Yuan for the FT–IR measurements.

Supporting Information Available: FTIR spectra, interfacial tension measurements, and thermogravimetric analysis of Janus particles. This material is available free of charge via the Internet at <http://pubs.acs.org>.

LA060693I